Three-Ring-Based Thermotropic Mesogens with a Dimethylamino Group: Structural Characterization, Photophysical Properties, and Molecular Order

ARTICLE *in* THE JOURNAL OF PHYSICAL CHEMISTRY C · APRIL 2015

Impact Factor: 4.77 · DOI: 10.1021/acs.jpcc.5b00630

6 AUTHORS, INCLUDING:

Guruprasad Reddy Mandadhi

CSIR - Central Leather Research Institute

2 PUBLICATIONS **0** CITATIONS

SEE PROFILE

Nitin P Lobo

Central Leather Research Institute

18 PUBLICATIONS **76** CITATIONS

SEE PROFILE

Easwaramoorthi Shanmugam

Central Leather Research Institute

32 PUBLICATIONS **482** CITATIONS

SEE PROFILE

Asit Baran Mandal

Central Leather Research Institute

360 PUBLICATIONS **3,201** CITATIONS

SEE PROFILE

THE JOURNAL OF PHYSICAL CHEMISTRY C

Article

pubs.acs.org/JPCC

Three-Ring-Based Thermotropic Mesogens with a Dimethylamino Group: Structural Characterization, Photophysical Properties, and Molecular Order

M. Guruprasad Reddy,[†] E. Varathan,[‡] Nitin P. Lobo,[§] S. Easwaramoorthi,[‡] T. Narasimhaswamy,*[,†] and A. B. Mandal[‡]

[†]Polymer Laboratory, [‡]Chemical Laboratory, and [§]Chemical Physics Laboratory, CSIR-Central Leather Research Institute, Adyar, Chennai 600020, India

Supporting Information

ABSTRACT: Thermotropic liquid crystals exhibiting light-emitting properties are gaining popularity as functional materials in view of their application in organic light-emitting diodes. Such mesogens essentially require active chromophoric moieties in the mesogenic core so that the mutual light-emitting and liquid crystalline properties can be realized. In this work, three-ring-core-based mesogens with a terminal dimethylamino unit are subjected to structural characterization by various techniques. These mesogens exhibit enantiotropic nematic as well as smectic A phase with interdigitated layer organization (SmA_d). This is a surprising observation because the SmA_d organization is commonly observed for calamitic mesogens with terminal polar groups. Interestingly, the single-crystal structure of the C_6 homologue indicates antiparallel packing. Furthermore, the photophysical properties of a representative C_{12} mesogen in solution disclose yet another exciting feature. The steady-state and time-resolved fluorescence studies indicate negative solvotochromism in solvents with differing polarity. To obtain greater insight, density functional theory (DFT)-based highest occupied molecular orbital−lowest unoccupied molecular orbital studies are carried out which support intramolecular charge-transfer interactions in this class of mesogens. Additionally, the DFT calculations also provide the ^{13}C chemical shifts which are compared with the solution NMR values for the structural assignment of all carbons in the core unit. Furthermore, the two-dimensional separated local field measurements for the C_{12} homologue in nematic and SmA_d mesophases offer $^{13}C-^{1}H$ dipolar couplings from which the molecular order is determined to be 0.59 and 0.70, respectively.

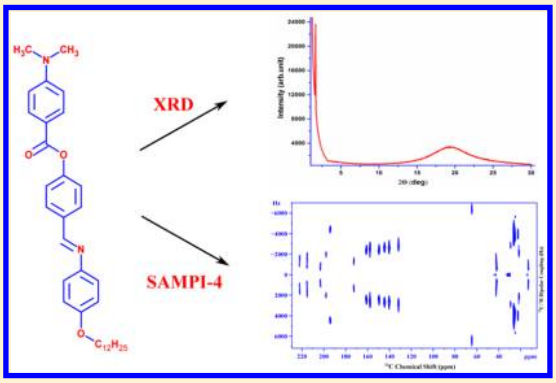

INTRODUCTION

Thermotropic liquid crystals are an important class of self-organized molecular entities which are in dynamic motion yet possess long-range orientational order.[1−3] The construction of liquid crystalline molecules is usually carried out by adopting a covalent strategy.[4−6] In recent years, use of noncovalent interactions, namely, hydrogen bonding, $\pi-\pi$ interactions, charge-transfer interactions etc., for the construction of liquid crystals has gained recognition.[7−9] In a noncovalent approach of building mesogens, the molecular core demands a terminal active functionality.[10] For example, in the case of hydrogen bonding-based mesogens, the core is designed to have a donor (carboxylic acid) or an acceptor (pyridine) as a vital part.[11,12] For those based on charge-transfer interactions, typically an electron-releasing group such as an *N*,*N*-dimethylamino moiety is preferred at terminal location.[13,14] Generally, charge-transfer complexes in liquid crystalline molecules are perceived between a donor and an acceptor, which could be either mesogenic or nonmesogenic.[15,16] In contrast, the intramolecular charge-transfer interactions of mesogens involving donor and acceptor as integral parts of the molecule are relatively less explored.[17] Quite remarkably, though the *N*,*N*-dimethylamino group is an excellent donor for charge-transfer interactions, for liquid crystalline properties, this moiety is considered to be less efficient owing to the orientation of CH_3 group of $-N(CH_3)_2$ away from the molecular plane.[18,19] In this context, it is curious to note that the insertion of polar groups like NO_2, CN at the terminal position of a core directly favor unusual smectic mesophases, which is attributed to the terminal dipoles that lead to antiparallel organization.[20−23] Thus, it is of considerable importance to undertake investigations dealing with *N*,*N*-dimethylamino-based mesogens in liquid crystalline phase to understand the molecular organization. In such mesogens, besides the liquid crystallinity, the other important properties such as charge-transfer complex and photoluminescence would be of significant interest because the π-conjugated organic

Received: January 21, 2015
Revised: March 27, 2015
Published: April 3, 2015

DOI: 10.1021/acs.jpcc.5b00630
J. Phys. Chem. C 2015, 119, 9477−9487

functional materials demand combination of these unusual features.[24,25] Hence, in this work, three-ring-based thermotropic mesogens with terminal *N*,*N*-dimethylamino moiety and alkoxy chain are synthesized and a comprehensive characterization is attempted using hot-stage optical polarizing microscopy (HOPM), differential scanning calorimetry (DSC), and single-crystal as well as powder X-ray diffraction (XRD) to realize the liquid crystalline properties and the molecular packing. Quite interestingly for a dodecyloxy mesogen, the XRD result suggests an interdigitated smectic layer organization which is a rare feature in *N*,*N*-dimethylamino-based mesogens. Furthermore, density functional theory (DFT) calculations are used to determing the geometry-optimized structure, highest occupied molecular orbital−lowest unoccupied molecular orbital (HOMO−LUMO) properties as well as ^{13}C NMR isotropic chemical shifts. Additionally, the photophysical properties of the C_{12} homologue is explored by performing steady-state as well as time-resolved fluorescence measurements.[26,27] In recent years, the solid-state ^{13}C NMR experiments, specifically, the two-dimensional (2D) separated local field (SLF) measurements in liquid crystalline phase have become popular in view of the wealth of information viz. the molecular order, molecular topology, and molecular dynamics offered by the technique.[28−32] Hence, the 2D SAMPI-4 experiments are also accomplished for determining the orientational order for a representative C_{12} mesogen in SmA_d and nematic phases.

EXPERIMENTAL SECTION

The compounds, namely, 4-(((4-(hexyloxy)phenyl)imino)-methyl)phenyl benzoate (HIMPDB), 4-(((4-dodecyloxy-phenyl)imino)methyl)phenyl4-(dimethylamino)benzoate (DdIMPDB), and 4-(((4-(dodecyloxy)phenyl)imino)methyl)-phenyl benzoate (DdPPB) were synthesized by multistep synthetic routes. The experimental protocols and the spectral data are provided in Supporting Information.

Instrumentation Details. Fourier transform infrared (FT-IR) spectra of the compounds were recorded on an ABB BOMEM MB3000 spectrometer using KBr pellets. ^1H and ^{13}C solution NMR spectra of the mesogens in $CDCl_3$ were acquired on a Bruker 400 MHz Avance III HD NanoBay NMR spectrometer. Typically, 0.5 mg of the sample was dissolved in 0.7 mL $CDCl_3$ at room temperature, and tetramethylsilane (TMS) was used as the internal standard. The resonance frequencies of ^1H and ^{13}C were 400.23 and 100.64 MHz, respectively. The nature of the mesophase and the temperature of occurrence were determined with an Olympus BX50 hot-stage optical polarizing microscope equipped with Linkam THMS 600 stage and TMS 94 temperature controller. The photographs were taken using an Olympus C7070 digital camera. Differential scanning calorimetry traces were recorded using a DSC Q200 instrument with a heating rate of 10 °C/min in nitrogen atmosphere. The data obtained from the second heating is considered for discussion. The single-crystal X-ray structure of HIMPDB was determined using a Bruker Kappa APEXII single-crystal X-ray diffractometer at SAIF, IIT-Madras, Chennai. UV−visible absorption spectra were measured using a Shimadzu UV-1800 spectrophotometer. The steady-state fluorescence measurements were carried out by a Varian Cary Eclipse fluorescence spectrophotometer, whereas the fluorescence lifetime decay profiles were measured by the time-correlated single photon counting method (IBH). The samples were excited at 375 nm laser (Tsunami, Spectra Physics), and the decay curves were monitored at respective emission maximum wavelength. The decay profiles were analyzed using DAS6 software and are fitted satisfactorily with a single exponential function.

Computational Details. The ground (S_0) geometries of DdIMPDB and DdPPB were optimized using a density functional theory-based method with Becke's three-parameter functional and the Lee−Yang−Parr functional (B3LYP)[33,34] with 6-31G* basis set. On the basis of the gas-phase optimized geometry of DdIMPDB and DdPPB, spectral properties in chloroform were calculated by time-dependent density functional theory (TD-DFT) method with the polarizable continuum model (PCM) at the B3LYP/6-31G* level of theory. All the calculations were carried out using the Gaussian 09 program package.[35]

Powder X-ray Measurements. Powder X-ray diffraction studies of the unoriented samples (Lindemann capillary; diameter of 1 mm; Hampton Research, Aliso Viejo, CA) were carried out using a PANalytical instrument (DY 1042-Empyrean) operating with a line focused Ni-filtered Cu Kα (λ = 1.54 Å) beam and a linear detector (PIXcel 3D). The sample temperature was controlled with a precision of 0.1 °C using a heater and a temperature controller (Linkam).[36,37]

Solid-State NMR Measurements. The solid-state NMR experiments were carried out on a Bruker Avance III HD 400 WB NMR spectrometer (9.4 T). ^1H and ^{13}C resonance frequencies were 400.07 and 100.61 MHz, respectively. The spectra in the liquid crystalline phases of the sample were recorded using a double-resonance 4 mm MAS WVT probe under static conditions. Because the liquid crystalline phase is observed at higher temperature for DdIMPDB, the sample is a fine powder at room temperature. Typically, 100 mg of the powder sample was taken in a 4 mm Zirconia rotor with Teflon spacer. The sample alignment was achieved by first heating to the isotropic phase and then slowly cooling to the respective mesophases. The 1D ^{13}C NMR spectra in SmA_d and nematic phases were obtained by cross-polarization (CP) scheme with a contact time of 3 ms; number of scans, 256; recycle delay, 8 s; and 62.5 kHz radio frequency (RF) field strength on both the ^1H and ^{13}C channels. High-resolution 2D SLF spectra were obtained under static conditions using the SAMPI-4 pulse sequence[38] (Figure S6 of Supporting Information) that correlates the ^{13}C chemical shift with the associated $^{13}C-^1H$ dipolar coupling. Experimental conditions for SAMPI-4 pulse scheme for liquid crystalline samples were described in our earlier work.[12,28,29,39] The CP contact time (τ) was 3 ms; the number of t_1 increments was 100, and the signal was acquired with 28 transients for each t_1 increment. To minimize RF heating effects, a recycle delay of 15s was used. The data were zero filled in both the t_2 and t_1 dimensions, yielding a 4096 × 256 real matrix. A shifted sine bell window function was applied to the time domain data, and the spectrum was processed in the phase sensitive mode. In all the experiments, SPINAL-64[40] with 30 kHz RF field strength was used to provide heteronuclear decoupling during the carbon signal acquisition. The sample temperature was regulated by a Bruker BVTB-3500 variable temperature unit and assessed from ^{207}Pb NMR chemical shift of Pb $(NO_3)_2$.[41] The ^{13}C chemical shift was externally referenced relative to the methine carbon of adamantane at 29.5 ppm.

DOI: 10.1021/acs.jpcc.5b00630
J. Phys. Chem. C 2015, 119, 9477−9487

RESULTS AND DISCUSSION

Scheme 1 shows the synthetic strategy adopted for preparing *N,N*-dimethylamino-based three-ring mesogens covered in this

Scheme 1

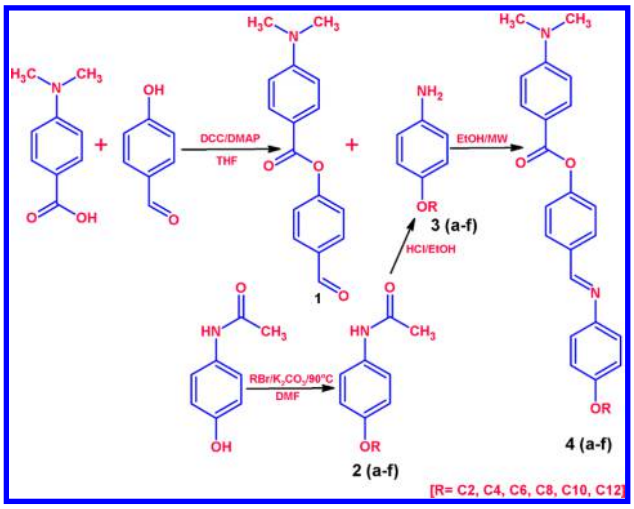

work. Accordingly, the target mesogens are achieved by condensing 4-*N,N*-dimethylaminobenzoyloxy benzaldehyde and 4-alkoxyanilines in ethanol under microwave conditions. The intermediate two-ring aldehyde is prepared by reacting 4-*N,N*-dimethylamino benzoic acid with 4-hydroxy benzaldehyde using DCC/DMAP in THF−DCM mixture at 0 °C. Consequently, the phenyl rings of the core are connected through ester and imine linking units while *N,N*-dimethylamino and alkoxy chains are positioned at terminal locations. When the length of the terminal alkoxy chain is varied from C_2 to C_{12} (even number carbons only), six mesogens are prepared. Figure 1 shows the DdIMPDB planar structure along with carbon

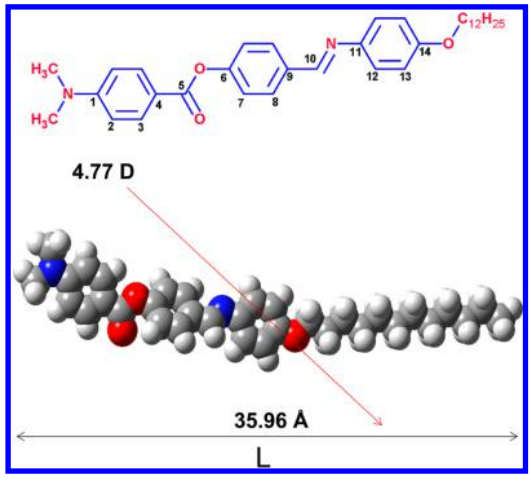

Figure 1. Molecular structure and energy-optimized space-filled model showing magnitude and direction of dipole moment of DdIMPDB.

numbers and the geometry-optimized structure from DFT. In addition, the direction and magnitude of the dipole moment (4.77 D) is shown for the geometry-optimized structure. Additionally, DFT is employed for determining the ^{13}C chemical shifts as well as examining the HOMO−LUMO levels to understand the photophysical properties of DdIMPDB. The ^{13}C NMR chemical shift values computed from DFT are compared with solution ^{13}C NMR values to complete the assignment of all the core unit carbons. Furthermore, the overall length of the molecule (*L*) is found to be 35.96 Å from the geometry-optimized structure. In addition, the structural identity of all the synthesized mesogens is established by FT-IR and ^{1}H and ^{13}C NMR spectral techniques (Figure S1−S3 of Supporting Information).

Mesophase Transitions and Molecular Organization. The liquid crystalline properties of the synthesized mesogens were carried out by HOPM and DSC methods, which revealed the occurrence of enantiotropic nematic phase for all the mesogens and an additional SmA_d phase for DdIMPDB. For instance, in HOPM, upon cooling the samples from isotropic phase, either schlieren texture or marble texture is seen for the nematic phase whereasa fan texture is clearly noticed for the SmA_d mesophase (Figure 2).[42] These observations are further

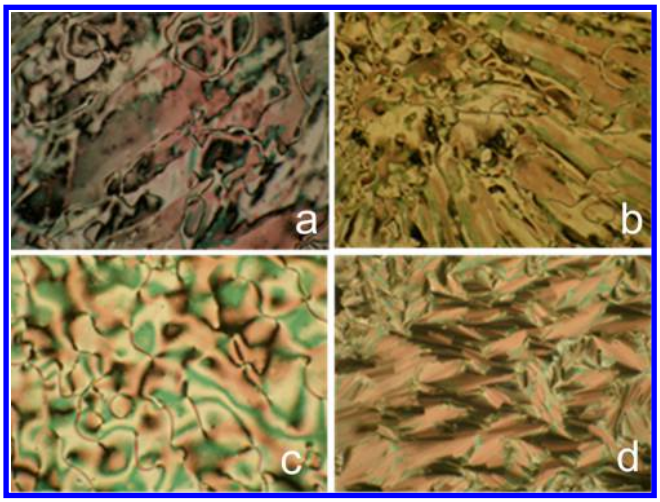

Figure 2. HOPM photographs of (a) nematic phase of BIMPDB at 250.1 °C, (b) nematic phase of HIMPDB at 228.8 °C, (c) nematic phase of OIMPDB at 225.5 °C, and (d) SmA_d phase of DdIMPDB at 170.8 °C.

established by DSC in which typical transitions associated with T_{C-N} and T_{N-I} are noticed for all the homologues (Figure S4 of Supporting Information) (Table 1). For DdIMPDB, an enantiotropic SmA_d mesophase is additionally observed in DSC scan (Figure 3). An examination of crystal-to-mesophase transition temperatures (Table 1) reveal that with increase in terminal chain length, a decrease in transition values is noticed, although the trend is not uniform across the homologues. The T_{N-I} values, on the other hand, showed a regular decrease with increase in terminal chain length.[43] Accordingly, the mesophase range for all the mesogens showed variation in the span of 60−90 °C. The good mesophase range suggests that the anisotropic molecular polarizability is high because of the presence of *N,N*-dimethylamino group, which is in conjugation with phenyl rings of the core unit.[43,44] To ascertain the molecular packing and geometry, the single-crystal structure of HIMPDB is determined. The XRD data indicates triclinic, *P*1 space group of the crystal structure with antiparallel packing (Figure 4b). The important features of the single-crystal data are listed in Table 2.

The powder X-ray diffraction of DdIMPDB in the temperature range of 120−190 °C is accomplished because it exhibits enantiotropic SmA_d phase in addition to nematic phase. Table 3 lists the *d* values measured from powder X-ray diffraction at

DOI: 10.1021/acs.jpcc.5b00630
J. Phys. Chem. C 2015, 119, 9477−9487

Table 1. Transition Temperatures and Enthalpy Values of Synthesized Mesogens (4a–f)

code	temperature $T_{C-N/C-SmAd}$	ΔH (K·cal/mol)	temperature T_{SmAd-N}	ΔH (K·cal/mol)	ΔT T_{SmAd-N}	temperature T_{N-I}	ΔH (K·cal/mol)	ΔT T_{N-I}
4a	182.7	7.28	–	–	–	255.6	0.33	66.7
4b	169.6	6.81	–	–	–	251.8	0.38	76.2
4c	148.7	6.84	–	–	–	236.7	0.31	88.0
4d	126.9	8.43	–	–	–	222.9	0.29	96.0
4e	133.2	9.06	–	–	–	211.9	0.22	78.7
4f	122.8	8.35	178.1	0.0096	53.3	209.5	0.18	31.4

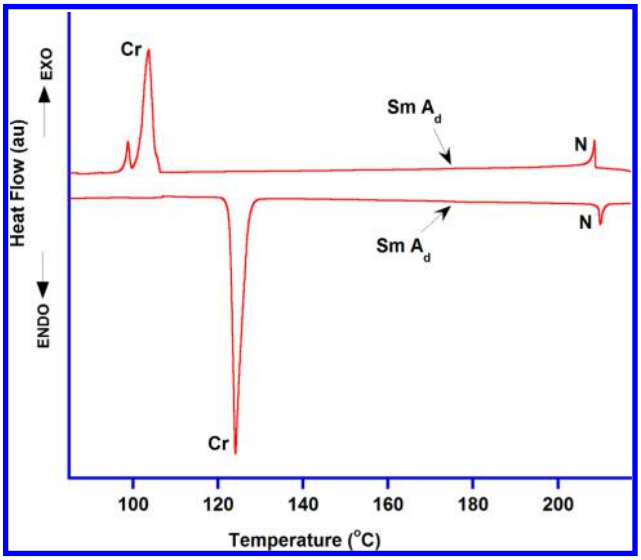

Figure 3. DSC second heating and cooling scans of DdIMPDB.

various temperatures in the smectic mesophase. The diffractogram at 150 °C (Figure 5) shows a sharp reflection in the small-angle region and a broad hump in the wide-angle region. The presence of sharp reflection in the small-angle region is characteristic of layer ordering of smectic phase while the broad hump in the wide-angle region indicates the absence of in-plane order and liquidlike nature of molecules in the layer (Figure 5).[45−47] Accordingly, the layer spacing, *d*, is found to be 53.44 Å at 150 °C. Table 3 lists the *d*/*L* ratio, where *L* is the length of the geometry-optimized DdIMPDB mesogen and *d* is the layer spacing measured from the diffractogram at various temperatures. It is clear from Table 3 that the *d*/ *L* ratio in the temperature range (120−190 °C) is found to be ∼1.46−1.51. These values distinctly suggest that the smectic phase is interdigitated bilayer smectic A type (SmA_d).[45−49] It is remarkable to note that *N*,*N*-dimethylamino-based mesogens usually show nematic phase.[5,50] The presence of SmA_d in DdIMPDB is an interesting observation because such an organization is normally encountered with mesogens possessing terminal polar groups like CN, NO_2, etc.[20−23,45−49] In contrast,

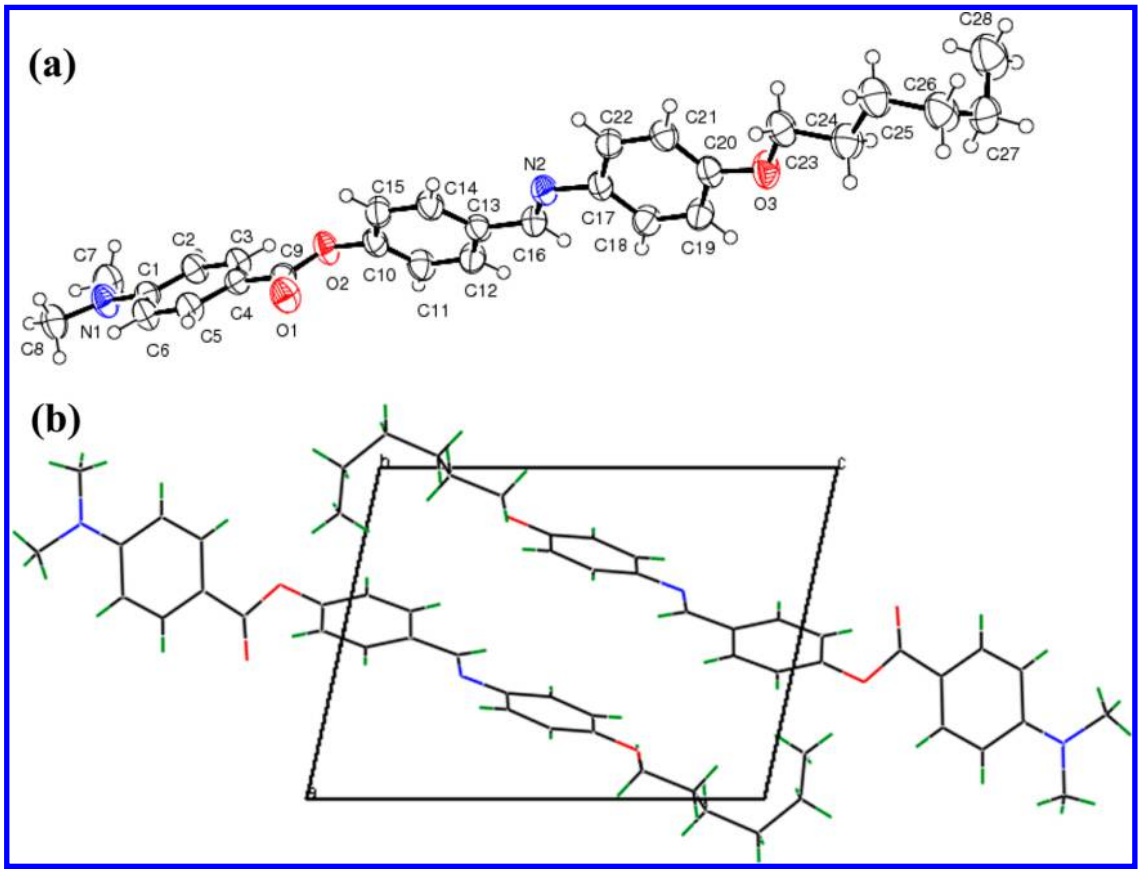

Figure 4. (a) ORTEP diagram of HIMPDB; (b) antiparallel packing of HIMPDB in crystal.

DOI: 10.1021/acs.jpcc.5b00630
J. Phys. Chem. C 2015, 119, 9477−9487

Table 2. Single-Crystal Data of HIMPDB

empirical formula	$C_{28}H_{32}N_2O_3$
formula weight	444.56
crystal system	triclinic
crystal size (mm)	0.35 × 0.35 × 0.30
space group	*P*1
a (Å)	9.6360(3)
b (Å)	10.8458(3)
c (Å)	12.5627(4)
α (Å)	100.934(2)
β (Å)	97.887(2)
γ (Å)	109.429(2)
V (Å^3)	1186.90(6)
Z	2
ρ_{calcd} (g cm^{-3})	1.244
F(000)	476
temperature (K)	293(2)
radiation MoK*α* *λ* (Å)	0.71073
goodness-of-fit on F^2	1.020
reflections collected/unique	20470/4188
data/restraints/parameters	4188/0/299
R (int)	0.0310
CCDC entry, 1044591	

Table 3. Powder X-ray Diffraction Data of DdIMPDB

temperature (°C)	d_1 (Å)	d_2 (Å)	d/L
190	52.61	4.65	1.46
170	52.60	4.63	1.46
160	53.44	4.62	1.48
150	53.44	4.60	1.48
140	53.44	4.59	1.48
130	54.30	4.56	1.51
120	54.30	4.53	1.51

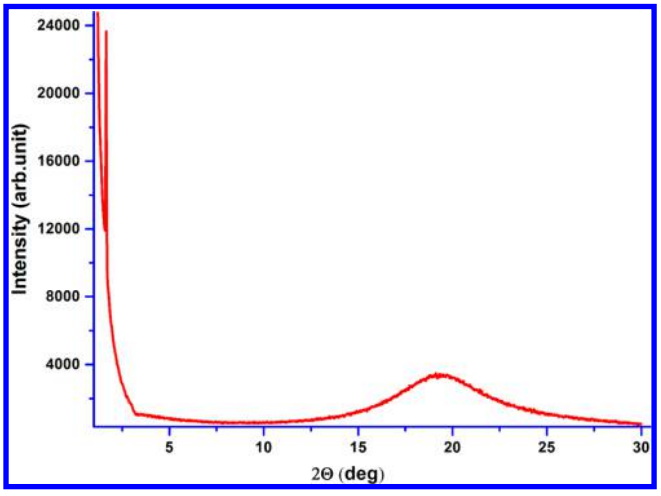

Figure 5. Powder X-ray diffraction profile for DdIMPDB at 150 °C.

in DdIMPDB, finding SmA_d phase with an electron-releasing *N*,*N*-dimethylamino group at the terminal position is a significant observation. Furthermore, it is generally noticed that in SmA_d, the molecules are preferred to be in antiparallel packing to compensate the net polarity.[20−23] It is important to note that the single-crystal structure of HIMPDB, a C_6 homologue, also shows antiparallel packing. Thus, it is quite likely that when DdIMPDB melts into smectic mesophase the antiparallel organization is preserved, as experimentally confirmed by XRD measurements.

Photophysical Properties in Solution. It has been established based on the photophysical studies that *N*,*N*-dimethylamino benzoates exhibit twisted intramolecular charge-transfer (TICT) interactions.[26,27,51,52] Because the mesogens under investigation are constructed from 4-dimethylamino benzoic acid, the photophysical properties of DdIMPDB in different solvents are investigated using steady-state and time-resolved fluorescence techniques.[53,54] Quite interestingly, the UV−visible absorption spectra of DdIMPDB (Figure 6)

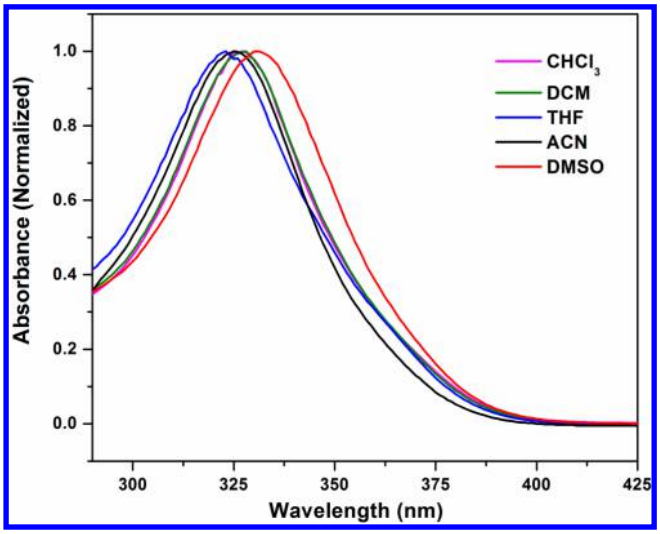

Figure 6. Solution absorption spectra of DdIMPDB in different solvents.

remains insensitive to the solvent polarity, whereas the fluorescence maxima are found to be fairly sensitive to the solvent polarity (Figure 7). Indeed, the fluorescence maximum

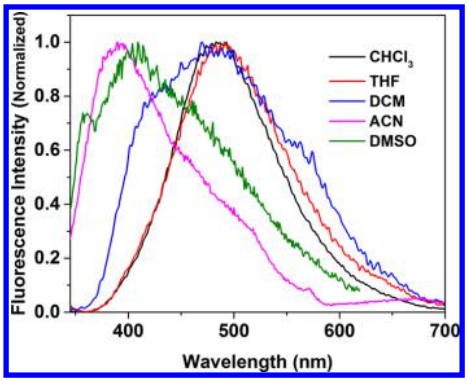

Figure 7. Solution fluorescence spectra of DdIMPDB in different solvents.

of DdIMPDB is found to be 480, 498, 475, 408, and 447 nm in chloroform, dichloromethane, tetrahydrofuran, acetonitrile and *N*,*N*-dimethyl sulfoxide solvents, respectively. This phenomenon is quite intriguing as the fluorescence maxima becomes blue-shifted with increase in solvent polarity which, is in sharp contrast to the behavior generally observed for *N*,*N*-dimethylaminobenzoates.[55] The negative solvatochromism in fluorescence witnessed for DdIMPDB is a rare observation, and most of the probes known to date exhibit negative solvatochromism in absorption rather than fluorescence. The

DOI: 10.1021/acs.jpcc.5b00630
J. Phys. Chem. C 2015, 119, 9477−9487

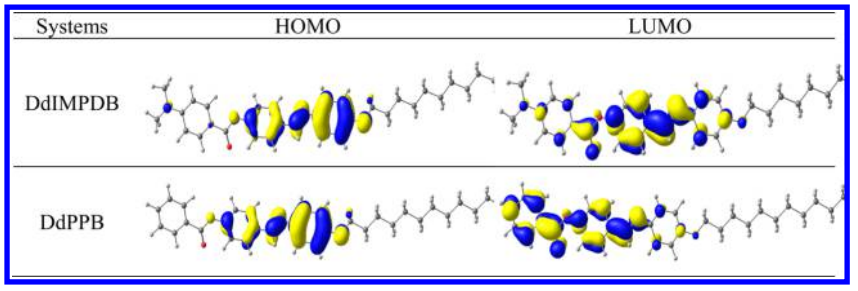

Figure 8. FMO distribution of DdIMPDB and DdPPB (isosurface value, 0.03 au) in $CHCl_3$ at PCM-B 3LYP/6-31G* level of theory.

Table 4. Summary of the Excited-State Electronic Transitions Obtained from the TD-DFT Calculations at B3LYP/6-31G* Level of Theory

compound	solvent	state	absorption (nm)	energy (eV)	oscillator strength (*f*)	dominant contribution (%)[a]	exptl. (nm)
DdIMPDB	$CHCl_3$	S_1	320.6	3.87	1.2034	H → L+1 (47%), H-1 → L (32%)	328
		S_2	281.0	4.41	0.9054	H → L+1 (34%), H-1 → L (16%)	
		S_3	205.2	6.04	0.2622	H → L+2 (32%), H-5 → L (32%)	
DdPPB	$CHCl_3$	S_1	320.5	3.87	0.9480	H → L (67%), H → L+1 (18%)	340
		S_2	266.3	4.66	0.6233	H-1 → L (38%),H-6 → L (28%)	

[a]H denotes HOMO and L denotes LUMO.

Stokes shift value calculated from the lowest-energy absorption and fluorescence maxima is 9750, 9690, 9900, 6460, and 7840 cm^{-1} in chloroform, dichloromethane, tetrahydrofuran, acetonitrile, and *N*,*N*-dimethyl sulfoxide solvents, respectively. The larger Stokes shift can be due to the significant structural changes that occur between the ground and excited state and to the intramolecular charge-transfer interactions. Nonetheless, the fluorescence lifetime remains almost constant ca. 1.14 ± 0.2 ns irrespective of the solvent used. In view of these interesting electronic properties of DdIMPDB, the nature of the electronic transition and frontier molecular orbital (FMO) distributions are investigated using density functional theory (DFT) at the B3LYP/6-31G* level of theory. The calculated FMO distributions of DdIMPDB are presented in Figure 8. It is evident from Figure 8 that for DdIMPDB, both HOMO and LUMO are localized on the benzylidene-phenyl unit. A close examination of these orbitals reveals that the HOMO is predominantly localized on the benzylidene-phenyl unit while the LUMO is mostly concentrated on the phenyl benzoate unit; *N*,*N*-dimethylaminobenzoate does not have any significant influence on the HOMO and LUMO. Thus, it can be concluded that the electronic properties of DdIMPDB could have originated from the benzylidene-phenyl rather than the *N*,*N*-dimethylaminobenzoate moiety. TD-DFT calculations presented in Table 4 have close agreement with experimental results. For the DdIMPDB, the maximum peak is predicted to be at 320.6 nm (f = 1.2034) which arises from the HOMO → LUMO+1 (47%) and HOMO−1 → LUMO (32%) transitions. To get clear insights on the role of *N*,*N*-dimethylamino group on electronic properties, the frontier molecular orbitals are also calculated for a hypothetical molecule DdPPB in which the terminal *N*,*N*-dimethylamino moiety is absent, wherein the LUMO is localized on the phenyl benzoate unit (Figure 8). A clear distinct feature in the LUMO for DdIMPDB and DdPPB suggests that pronounced charge transfer can be seen for the latter. The decrease in the magnitude of charge transfer in the presence of *N*,*N*-dimethylamino group could be attributed to its strong electron-donating behavior upon photoexcitation of DdIMPDB, which can also be responsible for the negative solvatochromism in fluorescence. The electron-transfer process from the *N*,*N*-dimethylamino group to benzylidene-phenyl is highly more favorable in polar solvents than the nonpolar solvents. The facile electron-transfer process in the polar environment probably destabilizes the excited state and leads to the negative solvatochromism in fluorescence. To confirm this hypothesis, the fluorescence spectra of DdPPB, which is a structural analogue of DdIMPDB, without the terminal *N*,*N*-dimethylamino group, is measured, which shows positive solvatochromism in fluorescence (Figure S5 of Supporting Information). On the basis of these facts, it can be concluded that the electronic properties of the DdIMPDB molecule originate from the benzylidene-phenyl moiety and the negative solvatochromism is due to the photoinduced electron transfer from dimethylamino group to benzylidene-phenyl of the core unit.

Solid-State ^{13}C NMR Spectroscopy. One of the synthesized mesogens, DdIMPDB, the C_{12} homologue, is investigated by high-resolution solid-state ^{13}C NMR in SmA_d and nematic mesophases. The static 1D and 2D ^{13}C NMR experiments are carried out in both phases with the purpose of finding the orientational order. The core unit carbons in the solution spectrum were assigned using ^{13}C chemical shifts calculated by the DFT method. This is a useful starting point for confirming the molecular structure and the assignment of the carbon peaks in the liquid crystalline phase. Figure 9a shows the proton decoupled ^{13}C NMR of DdIMPDB in $CDCl_3$ measured at room temperature. For the three-ring core unit carbons, 14 signals as listed in Table 5 are seen. For the terminal units, the methyl of *N*,*N*-dimethylamino carbon is noticed at 40 ppm and the methoxy carbon of dodecyloxy chain is observed at 68.3 ppm. The other methylene carbons of the terminal chain are seen in the range of 22−32 ppm, whereas methyl carbon showed a distinct signal at 14.2 ppm. It is also observed from the solution spectrum that the quaternary carbons showed low intensity in contrast to phenyl ring methine as well as imine methine carbons. The chemical shift assigned to core unit carbons of the mesogen are listed in Table 5. Among all the core unit carbons, the imine carbon is noticeable at 157 ppm. Thus, the solution ^{13}C NMR spectral

DOI: 10.1021/acs.jpcc.5b00630
J. Phys. Chem. C 2015, 119, 9477−9487

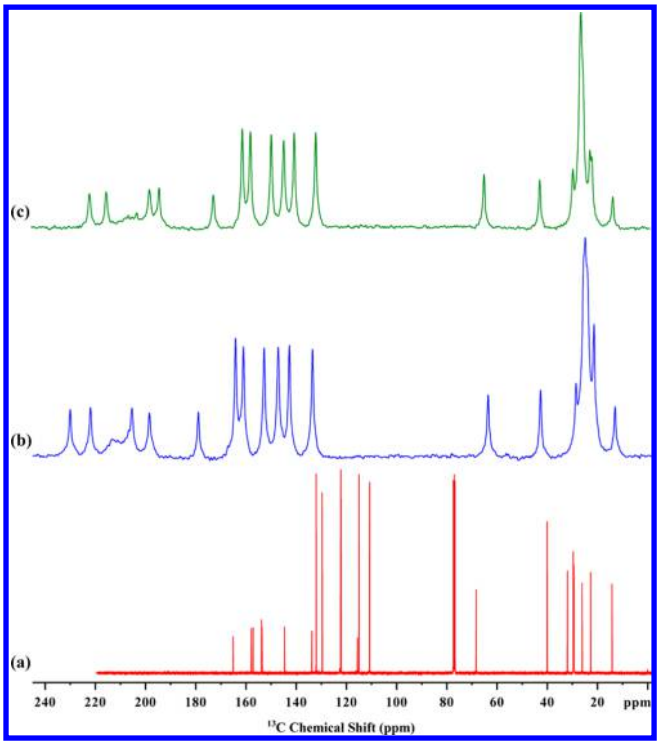

Figure 9. ^{13}C NMR spectra of DdIMPDB in (a) solution, (b) SmA_d phase at 145 °C, and (c) nematic phase at 195 °C.

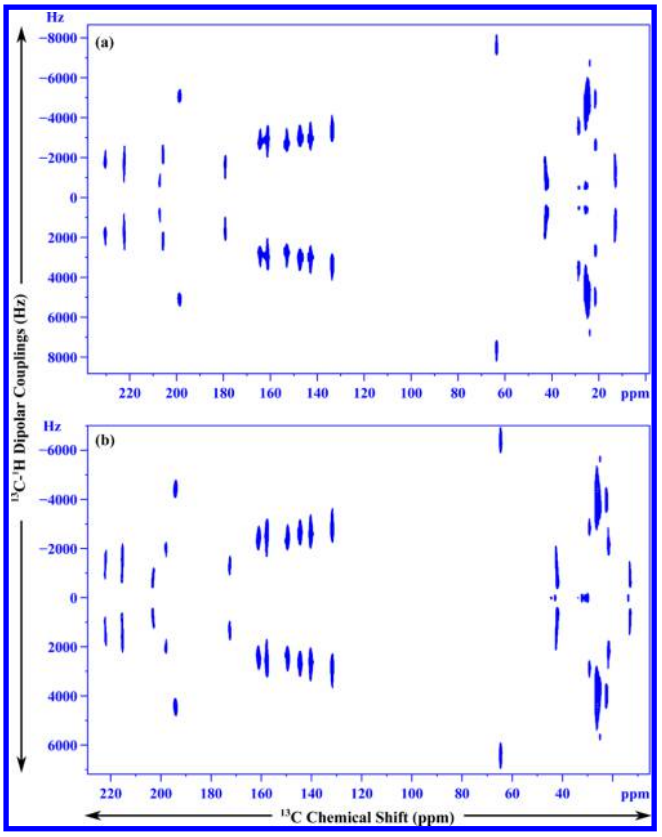

Figure 10. 2D SAMPI-4 spectra of DdIMPDB in (a) SmA_d phase at 145 °C and (b) nematic phase at 195 °C.

features of DdIMPDB are very much consistent with the molecular structure.

Panels b and c in Figure 9 show the static ^{13}C NMR spectra of DdIMPDB in SmA_d and nematic phases, respectively. The high resolution of the spectrum as well as the ^{13}C chemical shifts suggest the alignment of molecules in the magnetic field. The chemical shift assignment of the spectral lines in the mesophase is attempted by comparing the structurally similar segments of known liquid crystals and also making use of the 2D SAMPI-4 spectrum (Figure 10). For instance, 4-alkoxy benzylidene-based mesogens can provide the information about the chemical shift values of ring II carbons.[56] The assigned core unit carbons along with alignment-induced chemical shifts (AIS) are listed in Table 5. A clear increase in chemical shift values of core unit carbons in contrast to solution spectrum is noticed. For the terminal chain, a marginal decrease in chemical shifts is noted in liquid crystalline phase as against the solution. However, interestingly, for the *N*,*N*-dimethylamino carbons, an increase in chemical shift value is noticed in contrast to solution spectrum.[57] This is in stark difference to dodecyloxy chain, where decrease in chemical shifts of all the carbons is found in mesophase in contrast to the solution spectrum. The increase in chemical shift values of *N*,*N*-dimethylamino in the liquid crystalline phase could be due to different orientation of methyl group as against the terminal dodecyloxy chain. Because the

Table 5. ^{13}C NMR Data of DdIMPDB in Solution and Liquid Crystalline States

			145 °C			195 °C		
C no.	solution (ppm)	DFT (ppm)	SmA_d phase (ppm)	AIS (ppm)	^{13}C−^{1}H dipolar oscillation frequencies (kHz)	nematic phase (ppm)	AIS (ppm)	^{13}C−^{1}H dipolar oscillation frequencies (kHz)
1	153.8	149.8	222.1	68.3	1.64	215.1	61.3	1.34
2	110.8	108.2	133.5	22.7	3.28	131.6	20.8	2.78
3	132.1	133.1	164.3	32.2	2.84	160.9	28.8	2.42
4	115.6	117.0	179.0	63.4	1.55	172.5	56.9	1.21
5	165.2	161.0	207.1	41.9	0.79	203.0	37.8	0.71
6	153.6	154.4	222.1	68.5	1.64	215.1	61.5	1.34
7	122.4	120.8	152.8	30.4	2.75	149.3	26.9	2.39
8	129.7	130.6	161.0	31.3	2.90	157.7	28.0	2.50
9	133.8	132.7	205.6	71.8	2.20	197.9	64.1	1.91
10	157.3	152.6	198.6	41.3	5.00	194.0	36.7	4.33
11	144.7	145.3	205.6	60.9	1.50	197.9	53.2	1.25
12	122.2	127.9	147.2	25.0	2.99	144.3	22.1	2.62
13	115.0	116.9	142.8	27.8	2.98	140.2	25.2	2.59
14	157.9	157.6	230.3	72.4	1.61	221.8	63.9	1.33

DOI: 10.1021/acs.jpcc.5b00630
J. Phys. Chem. C 2015, 119, 9477−9487

Table 6. Planar Structure with Orienting Axis and Orientational Order Parameter Values of DdIMPDB

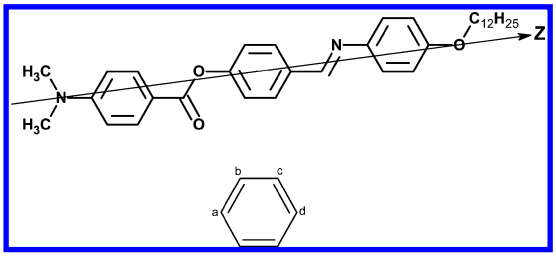

		angles				calculated dipolar oscillation frequencies (kHz)				
T (°C)	ring	θ_b	θ_c	S'_{zz}	$S'_{xx} - S'_{yy}$	b	c	a	d^a	RMSD (kHz)
145	I	118.8	120.2	0.68	0.070	3.28	2.84	1.54	1.57	0.05
	II	120.7	120.2	0.70	0.072	2.76	2.92	1.64	2.20	0.01
	III	119.5	119.6	0.68	0.066	3.03	3.00	1.55	1.55	0.04
195	I	118.7	119.9	0.57	0.056	2.76	2.44	1.28	1.31	0.06
	II	120.5	120.1	0.59	0.060	2.38	2.49	1.37	1.85	0.04
	III	119.2	119.4	0.57	0.054	2.61	2.56	1.29	1.29	0.03

[a]For carbon d in ring II, the contribution of the azomethine proton has also been taken into account.

methyl groups of *N*,*N*-dimethylamino group are away from the molecular axis, the orientation of the CSA tensors of methyl carbon is different from that of the dodecyloxy methyl carbon. Furthermore, in addition to 1D experiments, the 2D SLF experiments are also carried out for DdIMPDB in SmA_d and nematic phases. The 2D spectrum measured at 145 °C in SmA_d phase (Figure 10a) shows as many as 12 contours with varying intensities arising from protonated as well as nonprotonated carbons. The $^{13}C-^{1}H$ dipolar couplings of the core unit are listed in Table 5. The imine methine carbon showed a contour at 194 ppm in nematic phase (Figure 10b) with a $^{13}C-^{1}H$ dipolar coupling of 4.33 kHz. For the phenyl ring methine carbons, the $^{13}C-^{1}H$ dipolar couplings are in the range of ∼2.39−3.78 kHz, whereas for the quaternary carbons, the values are found to be ∼1.36−1.50 kHz. The 2D data also provides support for the assignment of core unit as well as terminal chain carbons because the separation of contours is guided by the orientation of individual C−H vectors. For instance, the identification of imine carbon is significantly easier from the 2D spectrum than from the 1D data alone. Similarly, the ester carbonyl assignment is straightforward because the $^{13}C-^{1}H$ dipolar coupling value would be less because it is away from neighboring protonated carbons. Also, the assignment of several methylene carbons of the dodecyloxy terminal chain in 2D is relatively easier than in the 1D spectrum (Figure 10). In SmA_d phase, the $^{13}C-^{1}H$ dipolar couplings as well as chemical shifts showed an increase in contrast to nematic phase due to increase in orientational order as SmA_d is more ordered than the nematic phase. The $^{13}C-^{1}H$ dipolar couplings (Table 5) determined from 2D experiments in both phases are utilized for finding the orientational order parameter.

The 2D SAMPI-4 provides dipolar oscillation frequencies from which the dipolar couplings can be extracted by adopting the established method.[12,28,29,58,59] These $^{13}C-^{1}H$ dipolar couplings are employed for finding the local orientational order parameter of the phenyl rings by the following equation.[59−61]

$$D_{CH} = K\left\{\frac{1}{2}(3\cos^2\theta_z - 1)S'_{zz} + \frac{1}{2}(\cos^2\theta_x - \cos^2\theta_y)(S'_{xx} - S'_{yy})\right\} \quad (1)$$

where $K = -h\gamma_H\gamma_C/4\pi^2 r_{CH}^3$; γ_H and γ_C are the gyromagnetic ratios of protons and carbons, respectively; r_{CH} is the internuclear distance between the carbon and proton nuclei; and θ_x, θ_y, and θ_z are angles that internuclear vector r_{CH} forms with the respective coordinate axes. The coordinate axes are the local axes defined on the molecular fragment under consideration; in this case, the phenyl ring is considered. The z axis is the para axis of the phenyl ring and the x axis is perpendicular and is in the plane of the ring. The standard bond distances employed for the calculations are r_{CH} = 1.1 Å for the C−H bond and r_{CC} = 1.4 Å for the C−C bond. During the fitting procedure, the two C−C−H bond angles have been slightly varied around 120° (assumed for an ideal hexagonal geometry) in view of the uncertainty involved in the position of the H atom as determined by X-rays.[58] Thus, the calculated S'_{zz} and $(S'_{xx} - S'_{yy})$ for each phenyl ring of the core in SmA_d and nematic phase, respectively, are listed in Table 6. Accordingly, S'_{zz} values of ring II in SmA_d and nematic phases are 0.70 and 0.59, respectively. These values are comparable with those of the calamitic mesogens that exhibit smectic A and nematic phases which are reported in the literature.[60−65] Based on the order parameter values of three phenyl rings in both nematic and SmA_d phases, the location of the long axis passing through the core can be identified. As explained in earlier work,[46] the ratios of order parameters of phenyl rings provide information about the angles between phenyl rings of the core unit. It is clear from Table 6 that in both phases, the order parameter of ring II is higher than that of ring I as well as that of ring III. This suggests that the long axis is more collinear to ring II than the other two rings. In a recent study, Domenici et al.[30] performed a ^{13}C NMR investigation of three-ring-based mesogen with a chiral center that exhibits S_A Devries phase and SmC* phase and calculated the order parameters employing ^{13}C chemical shifts as well as $^{13}C-^{1}H$ dipolar couplings (PDLF). Using $^{13}C-^{1}H$ dipolar couplings in three aromatic rings in SmA and in SmC* phases, the relative orientation of rings have been determined. Interestingly, in SmC* phase, the aromatic ring closer to the chiral lateral chain is found to be much more tilted than the other two rings, indicating the occurrence of a conformational change at the SmA−SmC* phase transition. This observation is supported by the order parameters which showed a decreasing trend in

DOI: 10.1021/acs.jpcc.5b00630
J. Phys. Chem. C 2015, 119, 9477−9487

SmC*. However, in the present investigation, though the mesogen exhibits SmA_d, no evidence for conformational change or anomaly in the order parameter values is noticed across the transition from nematic to SmC* phase. Furthermore, a plot of temperature and carbon chemical shifts (Figure S7 of Supporting Information) of all the core unit carbons support no abrupt change across the nematic-to-SmA_d phase transition. This suggests that the phase transition from nematic to SmA_d is not a first-order transition.[66,67] This observation is very well supported by the DSC data in which transition enthalpy associated with nematic-to-SmA_d phase is found to be low.

CONCLUSIONS

Thermotropic liquid crystals consisting of a three phenyl ring core with dimethylamino moiety and alkoxy chain as terminal units were synthesized from 4-*N*,*N*′-dimethylamino benzoic acid. The HOPM and DSC measurements confirmed the enantiotropic nematic mesophase for all the mesogens while SmA_d is additionally noticed for the C_{12} homologue. The XRD studies revealed interdigitation of molecules in the layers of SmA phase for the C_{12} homologue, wherein the d/L values were found to be in the range of ∼1.46−1.51. Furthermore, the photophysical properties of the C_{12} homologue in different solvents revealed negative solvatochromism in fluorescence emission. The DFT-based HOMO−LUMO calculations as well as steady-state and time-resolved fluorescence studies indicated intramolecular charge-transfer interactions. Additionally, HOMO−LUMO calculations revealed that the electronic properties of DdIMPDB originated from the benzylidene-phenyl moiety and the negative solvatochromism was due to the photoinduced electron transfer from dimethylamino group to benzylidene-phenyl of the core unit. The temperature versus ^{13}C chemical shifts plot suggested that the phase transition from nematic to SmA_d is of a second-order nature, which was well-supported by the ΔH values from the DSC measurements. The 2D SLF NMR experiments enabled the determination of the orientational order parameters in SmA_d and nematic phases. Based on the order parameter values of three phenyl rings in both nematic and SmA_d phases, the location of the long axis passing through the core was identified. Furthermore, the comprehensive characterization attempted in this investigation indicates that the mesogens under investigation are eligible candidates for organic light-emitting diode function. Thus, the present investigation clearly revealed many interesting findings such as appearance of SmA_d mesophase, antiparallel packing of molecules in crystal as well as smectic phase, negative solvatochromism in solution, and the second-order nature of the nematic-to-SmA_d phase transition. Therefore, it appears that the terminal dimethyamino group greatly influences many properties in this class of mesogens, as supported by the experimental data generated from a wide range of techniques.

ASSOCIATED CONTENT

Supporting Information

Synthesis details; FT-IR, ^1H NMR, and ^{13}C NMR spectral data of intermediates and final mesogens; figure of SAMPI-4 pulse sequence; DSC plot; fluorescence spectra; and plot of chemical shifts versus temperature. This material is available free of charge via the Internet at http://pubs.acs.org.

AUTHOR INFORMATION

Corresponding Author

*E-mail: tnswamy99@hotmail.com.

Notes

The authors declare no competing financial interest.

ACKNOWLEDGMENTS

The authors thank Prof. K. V. Ramanathan, NMR Research Centre, Indian Institute of Science, Bangalore, India for his support and keen interest in this work. The authors are thankful to Dr. V. Subramanian, CLRI, for the quantum chemical calculations. M.G.R. and T.N. are grateful to Prof. V. A. Raghunathan and Ms. K. N. Vasudha, Raman Research Institute, Bangalore, India for the powder X-ray measurements. We acknowledge the partial financial support from NWP-55, and M.G.R. thanks Council of Scientific and Industrial Research (CSIR), New Delhi for the financial support in the form of a Senior Research Fellow.

REFERENCES

(1) Kato, T.; Mizoshita, N.; Kishimoto, K. Functional Liquid-Crystalline Assemblies: Self-Organized Soft Materials. *Angew. Chem., Int. Ed.* **2006**, *45*, 38−68.

(2) Goodby, J. W.; Saez, I. M.; Cowling, S. J.; Gortz, V.; Draper, M.; Hall, A. W.; Sia, S.; Cosquer, G.; Lee, S.; Raynes, E. P. Transmission and Amplification of Information and Properties in Nanostructured Liquid Crystals. *Angew. Chem., Int. Ed.* **2008**, *47*, 2754−2787.

(3) Tschierske, C. Development of Structural Complexity by Liquid Crystal Self-Assembly. *Angew. Chem., Int. Ed.* **2013**, *52*, 8828−8878.

(4) Lehmann, M. Star-Shaped Mesogens − Hekates: The Most Basic Star Structure with Three Branches. *Top. Curr. Chem.* **2012**, *318*, 193−223.

(5) Eremina, A.; Jakli, A. Polar Bent-shape Liquid Crystals − From Molecular Bend to Layer Splay and Chirality. *Soft Matter* **2013**, *9*, 615−637.

(6) Demus, D. One Hundred Years of Liquid-Crystal Chemistry: Thermotropic Liquid Crystals with Conventional and Unconventional Molecular Structure. *Liq. Cryst.* **1989**, *5*, 75−110.

(7) Praefcke, K.; Singer, D. Charge Transfer Systems. In *Hand Book of Liquid Crystals*; Demus, D., Goodby, J., Gray, G. W., Spiess, H. W., Vill, V., Eds.; Wiley-VCH: Weinheim, Germany, 1998; Vol. *2B*, pp 945−967.

(8) Kumar, S. *Chemistry of Discotic Liquid Crystals: From Monomers to Polymers*; CRC Press, Taylor and Francis: Boca Raton, FL, 2011.

(9) Kato, T.; Frechet, J. M. J. A New Approach to Mesophase Stabilization Through Hydrogen Bonding Molecular Interactions in Binary Mixtures. *J. Am. Chem. Soc.* **1989**, *111*, 8533−8534.

(10) Kato, T.; Frechet, J. M. J. Development of Supramolecular Hydrogen-Bonded Liquid Crystals and its Impact on Liquid-Crystalline and Materials Science. *Liq. Cryst.* **2006**, *33*, 1429−1433.

(11) Paleos, C. M.; Tsiourvas, D. Supramolecular Hydrogen-Bonded Liquid Crystals. *Liq. Cryst.* **2001**, *28*, 1127−1161.

(12) Kesava Reddy, M.; Subramanyam Reddy, K.; Narasimhaswamy, T.; Das, B. B.; Lobo, N. P.; Ramanathan, K. V. $^{13}C-^1H$ Dipolar Couplings for Probing Rod-Like Hydrogen Bonded Mesogens. *New J. Chem.* **2013**, *37*, 3195−3206.

(13) Fukui, M.; Matsunaga, Y. Liquid Crystal Formation in Binary Systems. VII. Liquid Crystals Induced in N-[4-(Dimethylamino)-benzylidene]-4-alkoxyaniline-4,4′-Dinitrobiphenyl and Related Systems. *Bull. Chem. Soc. Jpn.* **1982**, *55*, 3707−3710.

(14) Shenoy, R. A.; Neubert, M. E.; Abdallah, D. G.; Keast, S. S.; Petschek, R. G. Synthesis and Mesomorphic Properties of 4-alkylamino-4′-substituted Diphenyl diacetylenes. *Liq. Cryst.* **2000**, *27*, 801−812.

DOI: 10.1021/acs.jpcc.5b00630
J. Phys. Chem. C 2015, 119, 9477−9487

(15) Imrie, C. T.; Karasz, F. E.; Attard, G. S. Side-Chain Liquid-Crystalline Copolymers containing Charge Transfer Groups. *Liq. Cryst.* **1991**, *9*, 47−57.
(16) Imrie, C. T.; Schleeh, T.; Karasz, F. E.; Attard, G. S. Dependence of the Transitional Properties of Polystyrene-based Side-Chain Liquid-Crystalline Polymers on the Chemical Nature of the Mesogenic Group. *Macromolecules* **1993**, *26*, 539−544.
(17) Chino, E.; Matsunaga, Y. Liquid Crystal Formation in Binary Systems. VIII. Induction of Smectic Phases by the Addition of 4-Alkoxynitrobenzene or 4-Alkoxy-benzonitrile to N-(4-propoxybenzylidine)-4-hexylaniline. *Bull. Chem. Soc. Jpn.* **1983**, *56*, 3230−3234.
(18) Collings, P. J.; Hird, M. *Introduction to Liquid Crystals Chemistry and Physics*; Taylor and Francis: London, 1997.
(19) Luckhurst, G. R.; Gray, G. W. *The Molecular Physics of Liquid Crystals*; Academic Press: New York, 1979.
(20) Hardouin, F. Exotism around the Smectic A State in Associated Liquid Crystals. *Phys. A(Amsterdam, Neth.)* **1986**, *140*, 359−367.
(21) Krishna Prasad, S.; Shankar Rao, D. S.; Sridevi, S.; Lobo, C. V.; Ratna, B. R.; Naciri, J.; Shashidhar, R. Unusual Dielectric and Electrical Switching Behavior in the De Vries Smectic A Phase of Two Organosiloxane Derivatives. *Phys. Rev. Lett.* **2009**, *102*, 147802−147805.
(22) Madhusudana, N. V. On the Polymorphism of the Smectic A Phases of Highly Polar Compounds. *Proc. Indian Acad. Sci., Chem. Sci.* **1983**, *92*, 509−525.
(23) Madhusudana, N. V. Liquid Crystals made of Highly Polar Compounds. *Braz. J. Phys.* **1998**, *28*, 301−313.
(24) O'Neill, M.; Kelly, S. M. Ordered Materials for Organic Electronics and Photonics. *Adv. Mater. (Weinheim, Ger.)* **2011**, *23*, 566−584.
(25) Akagi, K. *Handbook of Thiophene-based Materials: Applications in Organic Electronics and Photonics*; Perepichka, I. F., Perepichka, D. F., Eds.; John Wiley & Sons, Ltd.; Chichester, U.K., 2009.
(26) Lazarowska, A.; Józefowicz, M.; Heldt, J. R.; Heldt, J. Spectroscopic Studies of Inclusion Complexes of Methyl-*p*-dimethylaminobenzoate and its ortho derivative with α- and β- Cyclodextrins. *Spectrochim. Acta, Part A* **2012**, *86*, 481−489.
(27) Iwashita, Y.; Sugiyasu, K.; Ikeda, M.; Fujita, N.; Shinkai, S. TICT Induced Fluorescence Colour Change Actualized in an Organo Gel System. *Chem. Lett.* **2004**, *33*, 1124−1125.
(28) Lobo, N. P.; Das, B. B.; Narasimhaswamy, T.; Ramanathan, K. V. Molecular Topology of Three Ring Nematogens from ^{13}C-^{1}H Dipolar Couplings. *RSC Adv.* **2014**, *4*, 33383−33390.
(29) Kesava Reddy, M.; Varathan, E.; Lobo, N. P.; Das, B. B.; Narasimhaswamy, T.; Ramanathan, K. V. High-Resolution Solid State ^{13}C NMR Studies of Bent-Core Mesogens of Benzene and Thiophene. *J. Phys. Chem. C* **2014**, *118*, 15044−15053.
(30) Domenici, V.; Lelli, M.; Cifelli, M.; Hamplova, V.; Marchetti, A.; Veracini, C. A. Conformational Properties and Orientational Order of a De Vries Liquid Crystal Investigated through NMR Spectroscopy. *ChemPhysChem* **2014**, *15*, 1485−1495.
(31) *Thermotropic Liquid Crystals: Recent Advances*; Ramamoorthy, A., Ed.; Springer: Dordrecht, Netherlands, 2007.
(32) Dong, R. Y. *Nuclear Magnetic Resonance Spectroscopy of Liquid Crystals*; World Scientific: Singapore, 2010.
(33) Becke, A. D. Density Functional Thermochemistry. III. The Role of Exact Exchange. *J. Chem. Phys.* **1993**, *98*, 5648−5652.
(34) Lee, B.; Yang, W.; Parr, R. G. Development of Colle-Salvetti Correlation-Energy into a Functional of Electron Density. *Phys. Rev. B: Condens. Matter Mater. Phys.* **1988**, *37*, 785−789.
(35) Frisch, M. J.; Trucks, G. W.; Schlegel, H. B.; Scuseria, G. E.; Robb, M. A.; Cheeseman, J. R.; Scalmani, G.; Barone, V.; Mennucci, B.; Petersson, G. A.; et al. *GAUSSIAN 09*, revision A.02; Gaussian, Inc.: Wallingford, CT, 2009.
(36) Gupta, S. K.; Setia, S.; Sidiq, S.; Gupta, M.; Kumar, S.; Pal, S. K. New Perylene-based Non-Conventional Discotic Liquid Crystals. *RSC Adv.* **2013**, *3*, 12060−12065.
(37) Radhika, S.; Monika, M.; Sadasiva, B. K.; Roy, A. Novel Zigzag-Shaped Compounds Exhibiting Apolar Columnar Mesophases with Oblique and Rectangular Lattices. *Liq. Cryt.* **2013**, *40*, 1282−1295.
(38) Nevzorov, A. A.; Opella, S. J. Selective Averaging for High-Resolution Solid-State NMR Spectroscopy of Aligned Samples. *J. Magn. Reson.* **2007**, *185*, 59−70.
(39) Das, B. B.; Ajitkumar, T. G.; Ramanathan, K. V. Improved Pulse Schemes for Separated Local Field Spectroscopy for Static and Spinning Samples. *Solid State Nucl. Magn. Reson.* **2008**, *33*, 57−63.
(40) Fung, B. M.; Khitrin, A. K.; Ermolaev, K. An Improved Broad Band Decoupling Sequence for Liquid Crystals and Solids. *J. Magn. Reson.* **2000**, *142*, 97−101.
(41) Beckmann, P. A.; Dybowski, C. A Thermometer for Nonspinning Solid-State NMR spectroscopy. *J. Magn. Reson.* **2000**, *146*, 379−380.
(42) Dierking, I. *Textures of Liquid Crystals*; Wiley-VCH: Weinheim, Germany, 2003.
(43) Gray, G. W. *Molecular Structure and Properties of Liquid Crystals*; Academic Press: New York, 1962.
(44) Collings, P. J. *Liquid Crystals: Nature's Delicate Phase of Matter*; Princeton University Press: Princeton, NJ, 2002.
(45) Seddon, J. M. Structural Studies of Liquid Crystals by X-Ray Difraction. In *Hand Book of Liquid Crystals*; Demus, D., Goodby, J., Gray, G. W., Spiess, H.-W., Vill, V., Eds.; Wiley-VCH: Weinheim, Germany, 1998; Vol. *1*, pp 635−679.
(46) Kesava Reddy, M.; Subramanyam Reddy, K.; Yoga, K.; Prakash, M.; Narasimhaswamy, T.; Mandal, A. B.; Lobo, N. P.; Ramanathan, K. V.; Shankar Rao, D. S.; Krishna Prasad, S. Structural Characterization and Molecular Order of Rodlike Mesogens with Three- and Four-Ring Core by XRD and ^{13}C NMR Spectroscopy. *J. Phys. Chem. B* **2013**, *117*, 5718−5729.
(47) De Vries, A. The use of X-Ray Diffraction in the Study of Thermotropic Liquid Crystals with Rod-Like Molecules. *Mol. Cryst. Liq. Cryst.* **1985**, *131*, 125−145.
(48) Ostrovskii, B. I. Structure and Phase Transitions in Smectic A Liquid Crystals with Polar and Sterical Asymmetry. *Liq. Cryst.* **1993**, *14*, 131−157.
(49) Hardouin, F.; Sigaud, G.; Kellert, P.; Richard, H.; Nguyen, H. T.; Mauzac, M.; Achard, M. F. Smectic A Polymorphism from Low to High Molar Mass Systems. *Liq. Cryst.* **1989**, *5*, 463−478.
(50) Narasimhaswamy, T.; Srinivasan, K. S. V. Synthesis and Characterization of Novel Thermotropic Liquid Crystals containing a Dimethylamino Group. *Liq. Cryst.* **2004**, *31*, 1457−1462.
(51) Huang, W.; Zhang, X.; Ma, L. H.; Wang, C. J.; Jiang, Y. B. Intramolecular Charge Transfer Dual Fluorescence of Substituted-Phenyl *p*-Dimethylaminobenzoates with Comparable Electron Acceptors. *Chem. Phys. Lett.* **2002**, *352*, 401−407.
(52) Guo, R.; Kitamura, N.; Tazuke, S. Anomalous Solvent Effects on the Twisted Intramolecular Charge Transfer Fluorescence of Ethyl 4-(*N*,*N*-dimethylamino) benzoate in Chlorinated Solvents. *J. Phys. Chem.* **1990**, *94*, 1404−1408.
(53) Weisenborn, P. C. M.; Huizer, A. H.; Varma, C. A. G. O. Excited-State Dynamics of Ethyl 4-(*N*,*N*-dimethylamino) benzoate and Ethyl 4-(*N*,*N*-diethylamino) benzoate in Apolar and Polar Solvents. *J. Chem. Soc., Faraday Trans. 2* **1989**, *85*, 1895−1912.
(54) Weersink, R. A.; Wallace, S. C. Complexes of Methyl 4-(*N*,*N*-Dimethylamino) benzoate: Spectroscopy and Dynamics of the Charge Transfer State. *J. Phys. Chem.* **1994**, *98*, 10710−10719.
(55) Zhang, C. H.; Chen, Z. B.; Jiang, Y. B. Intramolecular Charge Transfer Dual Fluorescence of *p*-Dimethylaminobenzoates. *Spectrochim. Acta, Part A* **2004**, *60*, 2729−2732.
(56) Narasimhaswamy, T.; Lee, D. K.; Somanathan, N.; Ramamoorthy, A. Solid-State NMR Characterization of a Novel Thiophene-Based Three Phenyl Ring Mesogen. *Chem. Mater.* **2005**, *17*, 4567−4569.
(57) Narasimhaswamy, T.; Monette, M.; Lee, D. K.; Ramamoorthy, A. Solid-State NMR Characterization and Determination of the Orientational Order of a Nematogen. *J. Phys. Chem. B* **2005**, *109*, 19696−19703.

DOI: 10.1021/acs.jpcc.5b00630
J. Phys. Chem. C 2015, 119, 9477−9487

(58) Fung, B. M.; Afzal, J.; Foss, T. L.; Chau, M. H. Nematic Ordering of 4-*n*-alkyl-4′-cyanobiphenyls Studied by Carbon-13 NMR with Off-Magic-Angle Spinning. *J. Chem. Phys.* **1986**, *85*, 4808−4814.
(59) Xu, J.; Fodor-Csorba, K.; Dong, R. Y. Orientational Ordering of a Bent-Core Mesogen by Two-Dimensional ^{13}C NMR Spectroscopy. *J. Phys. Chem. A* **2005**, *109*, 1998−2005.
(60) Fung, B. M. ^{13}C NMR Studies of Liquid Crystals. *Prog. Nucl. Magn. Reson. Spectrosc.* **2002**, *41*, 171−186.
(61) Fung, B. M. Liquid Crystalline Samples: Carbon-13 NMR. *Encycl. Nucl. Magn. Reson.* **1996**, *4*, 2744−2751.
(62) Kalaivani, S.; Narasimhaswamy, T.; Das, B. B.; Lobo, N. P.; Ramanathan, K. V. Phase Characterization and Study of Molecular Order of a Three-Ring Mesogen by ^{13}C NMR in Smectic C and Nematic Phases. *J. Phys. Chem. B* **2011**, *115*, 11554−11565.
(63) Narasimhaswamy, T. Solid-state ^{13}C NMR Spectroscopy—A Powerful Characterization Tool for Thermotropic Liquid Crystals. *J. Indian Inst. Sci.* **2010**, *90*, 37−53.
(64) Domenici, V.; Geppi, M.; Veracini, C. A. NMR in Chiral and Achiral Smectic Phases: Structure, Orientational Order and Dynamics. *Prog. Nucl. Magn. Reson. Spectrosc.* **2007**, *50*, 1−50.
(65) Cifelli, M.; Domenici, V.; Marini, A.; Veracini, C. A. NMR Studies of the Ferroelectric SmC* Phase. *Liq. Cryst.* **2010**, *37*, 935−948.
(66) Jakli, A.; Saupe, A. *One and Two Dimensional Fluids−Physical Properties of Smectic Lamellar and Columnar Liquid Crystals*; Taylor and Francis, Boca Raton, FL, 2006.
(67) Oswald, P.; Pieranski, P. *Smectic and Columnar Liquid Crystals*; Taylor and Francis: Boca Raton, FL, 2006.

DOI: 10.1021/acs.jpcc.5b00630
J. Phys. Chem. C 2015, 119, 9477−9487